

# Accepted Manuscript

Research paper

Synthesis of Au(I) complex-based aqueous colloids for sensing of biothiols

Julia Elistratova, Bulat Faizullin, Nataliya Shamsutdinova, Aidar Gubaidullin, Igor Strel'nik, Vasily Babaev, Kirill Kholin, Irek Nizameev, Elvira Musina, Rafil Khairullin, Andrey Karasik, Asiya Mustafina

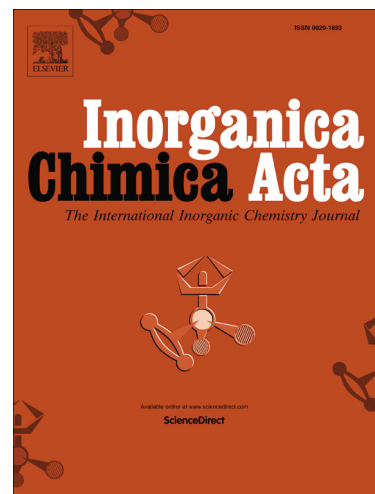
PII: S0020-1693(18)31393-8  
DOI: <https://doi.org/10.1016/j.ica.2018.10.006>  
Reference: ICA 18552

To appear in: *Inorganica Chimica Acta*

Received Date: 5 September 2018  
Revised Date: 3 October 2018  
Accepted Date: 3 October 2018

Please cite this article as: J. Elistratova, B. Faizullin, N. Shamsutdinova, A. Gubaidullin, I. Strel'nik, V. Babaev, K. Kholin, I. Nizameev, E. Musina, R. Khairullin, A. Karasik, A. Mustafina, Synthesis of Au(I) complex-based aqueous colloids for sensing of biothiols, *Inorganica Chimica Acta* (2018), doi: <https://doi.org/10.1016/j.ica.2018.10.006>

This is a PDF file of an unedited manuscript that has been accepted for publication. As a service to our customers we are providing this early version of the manuscript. The manuscript will undergo copyediting, typesetting, and review of the resulting proof before it is published in its final form. Please note that during the production process errors may be discovered which could affect the content, and all legal disclaimers that apply to the journal pertain.



## Synthesis of Au(I) complex-based aqueous colloids for sensing of biothiols.

Julia Elistratova<sup>a\*</sup>, Bulat Faizullin<sup>b</sup>, Nataliya Shamsutdinova<sup>a</sup>, Aidar Gubaidullin<sup>a</sup>, Igor Strel'nik<sup>a</sup>, Vasily Babaev<sup>a</sup>, Kirill Kholin<sup>a</sup>, Irek Nizameev<sup>a</sup>, Elvira Musina<sup>a</sup>, Rafil Khairullin<sup>b</sup>, Andrey Karasik<sup>a</sup>, Asiya Mustafina<sup>a</sup>

<sup>a</sup> Arbuzov Institute of Organic and Physical Chemistry, FRC Kazan Scientific Center of RAS, Arbuzov str., 8, 420088, Kazan, Russia

<sup>b</sup> Kazan (Volga region) Federal University, Kremlyovskaya str., 18, 420008, Kazan, Russia

\*Corresponding author: [969\\_969@bk.ru](mailto:969_969@bk.ru)

### Abstract

The present work represents new facile route for synthesis of luminescent hydrophilic core-shell colloids, where the luminescence results from Au(I) complex  $(\text{AuCl})_2\text{L}$  with cyclic PNNP ligand (L). The synthesis is based on solvent mediated aggregation of  $(\text{AuCl})_2\text{L}$  in aqueous organic solutions. Instability of  $(\text{AuCl})_2\text{L}$  in aqueous organic solutions was minimized by specific hydrophilic shell deposition arisen from electrostatically driven adsorption of polyethylenimine onto  $(\text{AuCl})_2\text{L}$ -based cores. Luminescence of the colloids is stable for week at least due to restricted degradation of the luminescent complex at the interface and high positive exterior charge of the colloids. The sensing properties of the colloids towards thiols results from their complex formation with  $\text{Au}^+$  ions. The thiol-induced stripping of  $\text{Au}^+$  ions from the colloids quenches the luminescence. The optimal conditions for fluorescent recognition of cysteine, homocysteine and glutathione with lower detection limits about  $1\mu\text{M}$  are highlighted in the work.

**Keywords:** Sensor Biothiols Luminescence Au(I) complex 1,5,3,7-diazadiphosphacyclooctane

### 1.Introduction

Heavy-metal complexes with  $d^{10}$  electron configuration have gained great attention during recent decades due to their unique photophysical characteristics, which makes them a good alternative to organic molecules in design of

nanosensors [1-3]. Unique electronic and spectral properties of Au(I) complexes are prerequisite for their particular importance among other  $d^{10}$ -complexes in sensing [4-8]. Solvent effect, interaction with substrates, phase transition or mechanistic influence are highlighted in literature as the reasons for switching or tuning of Au(I) complexes luminescence. Thus, unique sensing function of Au(I) complexes has been widely exemplified by different sensing procedures for recognition of vapors (vapochromism) and substrates in both organic and aqueous solutions [1-5].

High complexing ability of  $d^{10}$ -ions towards biomolecules, including thiols and biothiols can be considered as promising basis for their fluorescent recognition procedures. Biothiols play crucial role in human physiology due to their participation in biorelevant redox reactions. Cysteine and glutathione are well-known antioxidants able to prevent damage to cellular components caused by reactive oxygen species through redox transformations of the thiols to their oxidized disulfide forms. A high level of homocysteine in the blood makes a person more prone to endothelial cell injury, which leads to atherogenesis due to inflammation in the blood vessels. Thus, recognition of low molecular weight biothiols is very challenging task from biomedical point of view which has gained growing attention during recent decades. The literature procedures are mostly represented by organic dyes [6-11], gold or silver nanoparticles [12-19], which tend to change their luminescence under interaction with thiols. The thiol-induced luminescence response of both silver and gold nanoparticles commonly derives from their aggregation or de-aggregation induced by interfacial coordination of thiol molecules [12-19]. Since another biomolecules including peptides provide the similar effect on aggregation of the nanoparticles [20], combination of the nanoparticles with chemiluminescence-based assay was applied for more selective recognition of biothiols [21]. Thus, development of new sensors on the basis of Au(I) complexes is rather challenging task, although their wide application in aqueous solutions is greatly restricted by both low solubility and/or stability of such complexes in aqueous solutions. This problem can be solved by a synthesis of water soluble Au(I) complexes with a sensing function. However, a conversion of water insoluble complexes to hydrophilic nanosensors is worth noting as rather promising facile alternate to synthesis of Au(I)-based water soluble sensors.

Thus, the main goal of the present work is the development of facile synthetic route for conversion of the water insoluble Au(I) complex into selective hydrophilic nanosensor for luminescent recognition of thiols and biothiols. The recently represented Au(I) complex  $(\text{AuCl})_2\text{L}$  with cyclic PNNP ligand (L) was chosen as the subject of the present work due to its high stimuli responsive green luminescence with both vapochromism in solid state and solvatochromism in organic solutions [22, 23]. The report [23] highlights sensing properties of  $(\text{AuCl})_2\text{L}$  in organic solutions resulted from the ability of the complex to bind some alkylammonium cations or the solvent molecules in host-guest binding mode.

The present report represents very facile one-pot synthetic procedure for conversion of  $(\text{AuCl})_2\text{L}$  into aqueous hydrophilic colloids stabilized through an efficient adsorption of PEI. The colloid stabilization is discussed in a correlation with host-guest complex formation of  $(\text{AuCl})_2\text{L}$  with ammonium groups of PEI. Moreover, the performed measurements reveal PEI-stabilized colloids as efficient nanosensors for low molecular weight thiols and biothiols versus thioethers.

## 2. Experimental Section

### 2.1 Materials

Sodium chloride NaCl, ascorbic acid, polyethylenimine (PEI branched,  $\text{MM}_{\text{averaged}} = 25,000 \text{ Da}$ ) were purchased from Aldrich Chemistry, sodium dihydrophosphate anhydrous ( $\text{NaH}_2\text{PO}_4$ , 99%) was purchased from ACROS Organics, sodium ethylenediaminetetraacetate dihydrate ( $\text{Na}_2\text{EDTA}\cdot 2\text{H}_2\text{O}$ , 99%), L-cysteine, L-homocysteine, glutathione, DL-methionine, dithiothreitol, Dulbecco's Phosphate Buffered Saline (DPBS) and bovine serum albumin were purchased from Sigma-Aldrich. Tris-(hydroxymethyl)-aminomethane extra pure from Scharlau and MES hydrate 99% from ACROS Organics were also used as the buffers.

Dimethyl sulfoxide (DMSO, 99.7%) purchased from Sigma-Aldrich was used as solvent after the common purification by distillation.

Complex  $(\text{AuCl})_2\text{L}$ , where L is 1,5-bis (p-tolyl) -3,7-bis (pyridin-2-yl) -1,5-diaza-3,7-diphosphocyclooctane was synthesized according to the technique described in [22].

Polyelectrolyte-stabilized  $(\text{AuCl})_2\text{L}$ -based colloids ( $\text{PEI}-(\text{AuCl})_2\text{L}$ ) were synthesized by drop-wise addition of  $(\text{AuCl})_2\text{L}$  ( $C=2\text{mM}$ ) in DMSO solution (2 mL) by syringe pump (dropping speed of 0.35 mL/min) into aqueous solution (8 mL) of polyelectrolyte PEI (1 g/L) and NaCl (0.5 M) at pH 6.85 under the vigorous stirring. These conditions favor the precipitation of  $(\text{AuCl})_2\text{L}$  species and their colloid stabilization by PEI adsorption. Obtained aqueous colloid was subjected to ultrasonic dispersion for 30 minutes (the temperature of the water in the ultrasonic bath, unless otherwise specified, was maintained at  $22 \pm 2^\circ \text{C}$ ). Then colloid phase was separated from supernatant by the centrifugation (10,000 rpm for 15 minutes) in order to work off an excess of PEI and NaCl. After separation of the supernatant deionized water was added to the precipitate to adjust the concentration of  $(\text{AuCl})_2\text{L}$  to 0.4 mM. This system was further subjected to ultrasonic dispersion for 30 minutes.

For the luminescent titration of  $\text{PEI}-(\text{AuCl})_2\text{L}$  colloids the initial solutions of substrates (ascorbic acid, L-cysteine, dithiothreitol, glutathione, DL-methionine) (20 mM) were prepared.

## 2.2 Methods

**Dynamic light scattering (DLS) and electrokinetic potential experiments** were performed by means of the Malvern Mastersize 2000 particle analyzer at  $25^\circ \text{C}$ . Electrokinetic potential values were calculated by the Smoluchowski-Helmholtz equation [24]. Experimental autocorrelation functions were analyzed with the Malvern DTS software and the second-order cumulant expansion methods. The average error was ca. 4%. All samples were prepared in deionized water filtered through PVDF membrane with a Syringe Filter (0.45  $\mu\text{m}$ ). All measurements were performed at least in triplicate at  $25^\circ \text{C}$ .

**pH-Measurements** were carried out on a pH-meter of InoLab pH-720 with a SenTix Mic pH-electrode (WTW). The instrument was calibrated using three standard buffer points (pH 4.01, 7.01 and 10.01).

**Luminescence spectra.** Luminescence spectra recorded on a spectrofluorometer FL3-221-NIR (Horiba Jobin Yvon) using 10 mm quartz cuvettes. Excitation of samples was performed at 365 nm and emission was detected at 400–650 nm, excitation and emission slits were 7 nm.

**Transmission electron microscopy (TEM).** TEM images were obtained by use of Hitachi HT7700 (Japan) at an accelerating voltage of 100 kV.

**Electrospray ionization mass spectrometry (ESI)** was applied using an AmaZon X ion trap mass spectrometer in positive mode.

**X-ray powder diffraction (PXRD)** measurements were performed on a Bruker D8 Advance diffractometer equipped with a Vario attachment and Vantec linear PSD, using Cu radiation (40 kV, 40 mA) monochromated by a curved Johansson monochromator ( $\lambda$  Cu  $K_{\alpha 1}$  1.5406 Å). Room-temperature data were collected in the reflection mode with a flat-plate sample. Sample was applied in liquid form on the surface of a standard zero diffraction silicon plate. After drying the layer, a few more layers were applied on top of it to increase the total amount of the sample. The sample was kept spinning (15 rpm) throughout the data collection. Patterns were recorded in the  $2\theta$  range between  $3^\circ$  and  $105^\circ$ , in  $0.008^\circ$  steps, with a step time of 0.1–5.0s. Several diffraction patterns in various experimental modes were collected for the samples. Processing of the data obtained was performed using EVA [25] and TOPAS [26] software packages. The PDF-2 powder X-ray diffraction database (ICDD PDF-2, Release 2011-2016) was used to identify the crystalline phase.

**Inductively Coupled Plasma Optical Emission Spectrometry (ICP-OES)**. Au were identified in the colloids using simultaneous inductively coupled plasma optical emission spectrometry (ICP-OES) model iCAP 6300 DUO by Varian Thermo Scientific Company equipped with a CID detector. This spectrometer enables the simultaneous measurement of peak heights within the 166 to 867 nm range. The optical resolution is less than 0.007 nm to 200 nm. The working frequency is 27.12 MHz. Together, the radial and axial view configurations enable optimal peak height measurements with suppressed spectral noises. Concentration of Au ions was determined by the spectral line 242.795 nm.

### 3. Results and discussion

#### 3.1. Synthesis of hydrophilic $(AuCl)_2L$ -based colloids

Literature data introduce a plenty of synthetic routes for conversion of water insoluble complexes into hydrophilic nanosized colloids. Commonly, they are based on the well-known core-shell morphology, where water insoluble

complex species form the hard cores, which are coated by hydrophilic shell. A choice of an optimal procedure for  $(\text{AuCl})_2\text{L}$  is greatly affected by its inconvenient stability in acidic and alkaline media. Thus, a hydrophilization of  $(\text{AuCl})_2\text{L}$  via polymeric or silica coating is an inconvenient route due to the complex degradation. The application of the solvent-mediated bottom-up approach which results in formation of hard cores with their subsequent non-covalent hydrophilic coating enables to obtain stable hydrophilic colloids without any degradation of the complex. This procedure was previously successfully applied for the efficient conversion of water insoluble lanthanide complexes into hydrophilic colloids for sensing and imaging [27-30]. The adsorption of polyelectrolytes onto charged hard cores provides very good opportunity for their colloid stabilization.

As it has been above mentioned the water insolubility of the complex is the main reason for its solvent-mediated conversion into hard templates for further polyelectrolyte deposition. The previously reported synthetic route for the conversion of water insoluble lanthanide complexes to polyelectrolyte-stabilized nano-colloids is based on precipitation of water insoluble particles under a drop-wise addition of the complex in organic solution to an aqueous solution of polyelectrolyte [27-30]. Thus, the modification of the previously reported procedure should be started from developing of convenient conditions for a solvent-mediated precipitation of nanosized species of  $(\text{AuCl})_2\text{L}$  complex. The drop-wise pouring of  $(\text{AuCl})_2\text{L}$  complex in the organic (DMSO, DMF and acetonitrile) solution to water results in the lack of precipitation. ESI measurements reveal the appearance of  $[(\text{Au}_2\text{Cl})\text{L}]^+$  in aqueous solution (Fig.1), which reveals the dissociation of  $(\text{AuCl})_2\text{L}$  to  $[(\text{Au}_2\text{Cl})\text{L}]^+$  and  $\text{Cl}^-$  (1) as the reason for the dissolution of  $(\text{AuCl})_2\text{L}$  instead of its precipitation in aqueous organic solution.



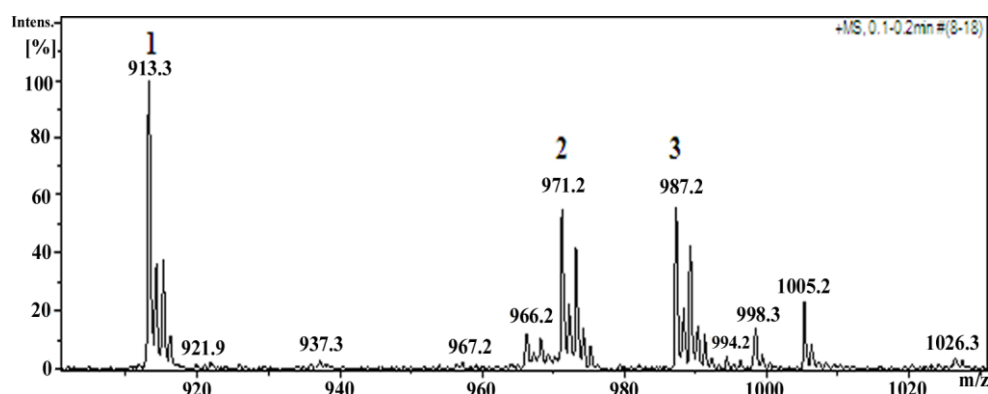
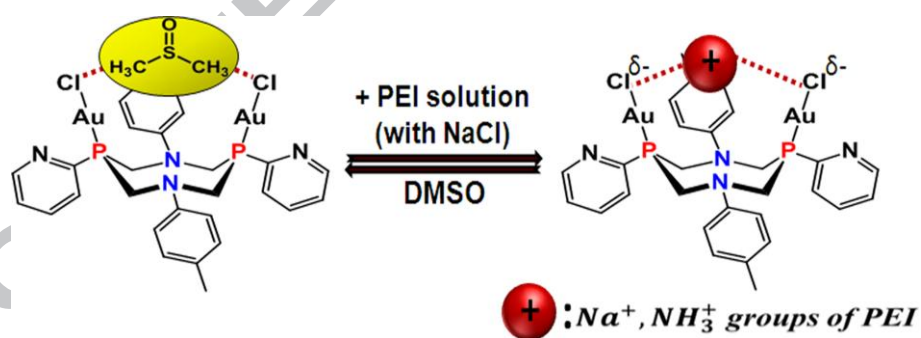


**Fig. 1.** ESI mass spectrum of the aqueous DMSO solution resulted from mixing DMSO solution of  $(\text{AuCl})_2\text{L}$  with water: 1- $[\text{Au}_2\text{CIL}]^+$ , 2- $[(\text{AuCl})_2\text{LNa}]^+$ , 3- $[(\text{AuCl})_2\text{LK}]^+$ .

Thus, excess amounts of  $\text{Cl}^-$  anions can shift the dissociation equilibrium (1) towards water insoluble  $(\text{AuCl})_2\text{L}$ . However, the peaks corresponding to  $[(\text{AuCl})_2\text{LM}]^+$ , where  $\text{M}=\text{Na}$  and  $\text{K}$  (Fig.1), point to efficiency of electrostatic interactions of sodium and potassium ions with pre-organized P-Au-Cl moieties of  $(\text{AuCl})_2\text{L}$  in accordance with Scheme 1. Therefore, host-guest complex formation of  $(\text{AuCl})_2\text{L}$  with sodium ions in  $\text{NaCl}$  solutions can provide additional stabilization of the complex.



**Scheme 1**

Indeed, 0.5 M of  $\text{NaCl}$  is optimal to get detectable by a naked eye precipitation of  $(\text{AuCl})_2\text{L}$  when its organic solution is mixed with aqueous solution of sodium chloride. The optimized procedure (detailed description is in Exp. Section) is based on the precipitation of  $(\text{AuCl})_2\text{L}$  under mixing its DMSO solution with aqueous solution of sodium chloride and polyethylenimine (PEI) at pH 6.85, where the latter provides a hydrophilic stabilization of the precipitated colloid species. DMSO was chosen as organic solvent due to the significant solubility of  $(\text{AuCl})_2\text{L}$  in DMSO and miscibility of the latter with water. The use of acetonitrile

and DMF solutions in the synthetic procedure is also possible, although the use of DMSO favors the stability of the hydrophilic colloids. The synthesized PEI-stabilized colloids were separated from the supernatant in order to work off excess amount of PEI and washed by water for several times. It is worth noting that the synthesized hydrophilic colloids are easy to manipulate by centrifugation-assisted phase separation for washing and controlling the colloids concentration. Electrokinetic potential and dynamic light scattering measurements of the synthesized colloids were performed after their redispersion in water. The results provide clear indication of the positively charged exterior layer of PEI-stabilized  $(\text{AuCl})_2\text{L}$ -based colloids (Fig. 2), which will be further designated as PEI- $(\text{AuCl})_2\text{L}$ . The measured electrokinetic potential of precipitated  $(\text{AuCl})_2\text{L}$ -based colloid species in the saline aqueous DMSO solution is negative (Fig. 2).

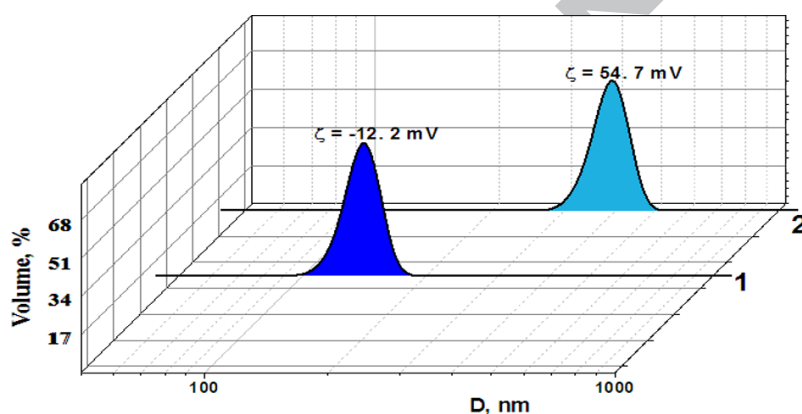


**Fig. 2.** Size distribution by volume in saline aqueous DMSO solutions of  $(\text{AuCl})_2\text{L}$  (1) and in PEI- $(\text{AuCl})_2\text{L}$  measured by DLS along with electrokinetic potential values ( $\zeta$ , mV) designated at the top of the peaks.

The ability of  $(\text{AuCl})_2\text{L}$  molecule to bind cations explains the efficiency of the interfacial adsorption of PEI onto the precipitated species, where ammonium groups of PEI can be bound with Au-P-Cl moieties at the interface of  $(\text{AuCl})_2\text{L}$ -based cores. Scheme 1 illustrates the binding mode between  $(\text{AuCl})_2\text{L}$  and ammonium groups of PEI.

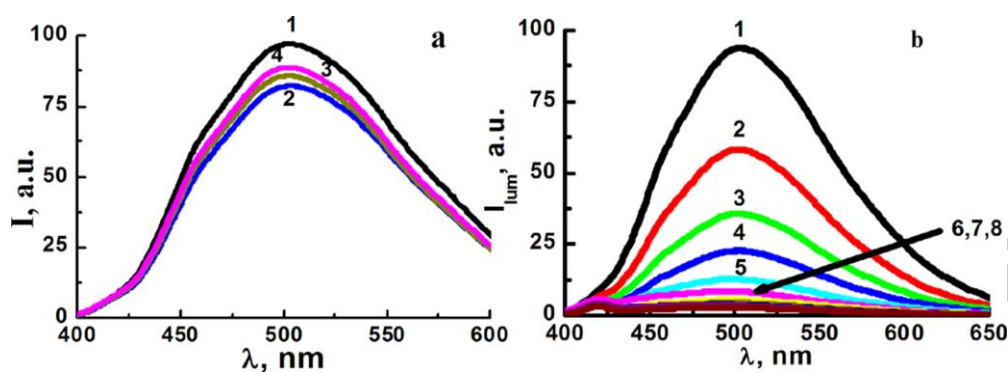


**Fig. 3.** Emission spectra of PEI-(AuCl)<sub>2</sub>L (0.4 mM) colloids measured: (a) exactly after their preparation (1) and under their storage within 2 (2), 4 (3) and 9 (4) days; (b) before (1) and after addition of various amounts of L-cysteine,  $\lambda_{\text{ex}}=365$  nm.

Taking into account that PEI solutions are highly alkaline the adjusting of pH to neutral range (5.6-6.0) is the important prerequisite of the successful synthetic procedure. Analysis of the supernatant solutions reveal very small concentration of Au (for more details see Suppl. Mat.). The losses of the complex during its conversion to the colloids is about 1%, which confirms the efficiency of (AuCl)<sub>2</sub>L precipitation in the applied synthetic conditions. The emission spectrum of the colloids similar with that of (AuCl)<sub>2</sub>L in DMSO solutions possesses one widened band with the maximum wavelength at about 505 nm under the excitation at 365 nm (Fig. 3 and Fig.S1 in Suppl. Mat.). The emission band arises from the Au(I)-disturbed ligand-centered luminescence [23]. Dynamic light scattering measurements reveal the averaged size at 380 nm with rather wide size distribution in PEI-(AuCl)<sub>2</sub>L colloids, while TEM images of the dried samples (Fig.4) reveal ultra-small sizes of the hard templates for PEI-(AuCl)<sub>2</sub>L. Such deviation between the size values revealed by DLS and TEM methods derives from the difference of the applied techniques. In particular, TEM images of the dried samples reveal the size of the hard (AuCl)<sub>2</sub>L-based templates, while DLS data indicate the size of the hydrated polyelectrolyte layer. The aggregation behavior of the colloids is worth noting as another factor influencing the size values revealed from the DLS measurements. This tendency is rather anticipated for the colloids synthesized in such saline conditions (0.5 M of NaCl), because the aggregation behavior of polyelectrolyte-stabilized colloids is greatly assisted by an exterior charge neutralization due to a counter-ion binding [31].

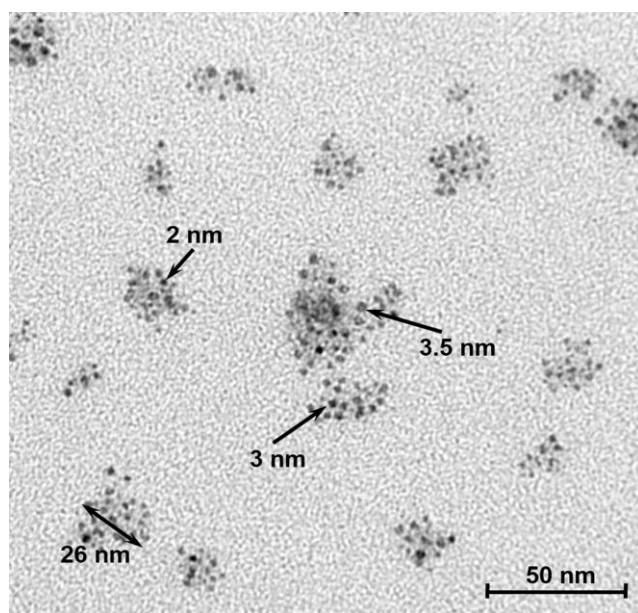


**Fig. 4.** TEM image of dried PEI-(AuCl)<sub>2</sub>L colloids.

The disproportionation of (AuCl)<sub>2</sub>L to Au<sup>0</sup> and Au<sup>3+</sup> was previously revealed for organic solutions of (AuCl)<sub>2</sub>L under their irradiation by sunlight [23], which results in the degradation of (AuCl)<sub>2</sub>L emission within few hours in organic solutions. It is worth noting that the luminescence of the synthesized aqueous colloids remains unchanged for nine days at least (Fig.3a). Thus, conversion of DMSO-based solutions of (AuCl)<sub>2</sub>L to PEI-(AuCl)<sub>2</sub>L colloids increases the complex stability.

PXRD data of the dried samples of PEI-(AuCl)<sub>2</sub>L reveal a crystallinity of the hard cores inside the polyelectrolyte coating, although the crystal structure of the colloids differs from that in the crystals obtained from DMSO solutions of (AuCl)<sub>2</sub>L (Figure 5). Our previous report is worth noting for highlighting the nucleophilic binding site of (AuCl)<sub>2</sub>L derived from two pre-organized P-Au-Cl moieties as the main reason for formation of solvato-complexes in DMSO solutions of (AuCl)<sub>2</sub>L [23]. The bound DMSO molecules can be easily substituted by sodium ions or alkylammonium groups of PEI molecule in the aqueous PEI-(AuCl)<sub>2</sub>L colloids (Scheme 1). The previously reported X-ray results [22, 23] indicate that the host-guest binding of (AuCl)<sub>2</sub>L with solvent molecules significantly affects the crystal packing in (AuCl)<sub>2</sub>L-based solvates. Fig. S2 in Suppl. Mat. illustrates the similarity in the PXRD patterns for the isostructural crystal solvates of (AuCl)<sub>2</sub>L with DMSO and acetone.

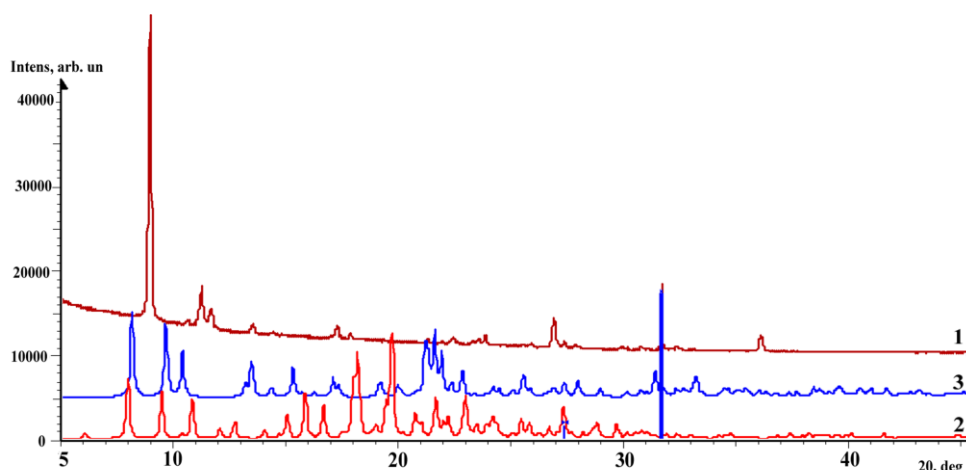


**Fig. 5.** Experimental diffraction pattern of the dried PEI-[(AuCl)<sub>2</sub>L] colloids (1), and calculated diffraction patterns of ligand L (2) and the complex grown from DMSO (3). Blue vertical lines show the position of the interference peaks corresponding to a crystalline NaCl, Ref.№ 01-070-2509 in the PDF-2 database.

Thus, the host-guest binding of cations or cationic moieties of polyelectrolyte with (AuCl)<sub>2</sub>L molecules at the interface of the colloid species can be the reason for specific crystal packing of the complex within nanosized colloid species. For this reason, the diffraction pattern of dried PEI-(AuCl)<sub>2</sub>L was examined and compared with that of (AuCl)<sub>2</sub>L·2DMSO, which is the crystal solvate of (AuCl)<sub>2</sub>L with DMSO (Figure 5). The presence of the peaks deriving from crystalline NaCl in the dried sample of PEI-(AuCl)<sub>2</sub>L is rather anticipated due to the saline synthetic conditions. These peaks do not interfere with the diffraction pattern of (AuCl)<sub>2</sub>L, which is quite different from the pattern of (AuCl)<sub>2</sub>L·2DMSO calculated from the single crystal X-ray data. This result indirectly confirms the substitution of DMSO molecule from the nucleophilic binding site of (AuCl)<sub>2</sub>L by cations (Na<sup>+</sup> or ammonium groups of PEI). The substitution is schematically illustrated by Scheme 1.

### 3.2. Substrate-induced luminescence response

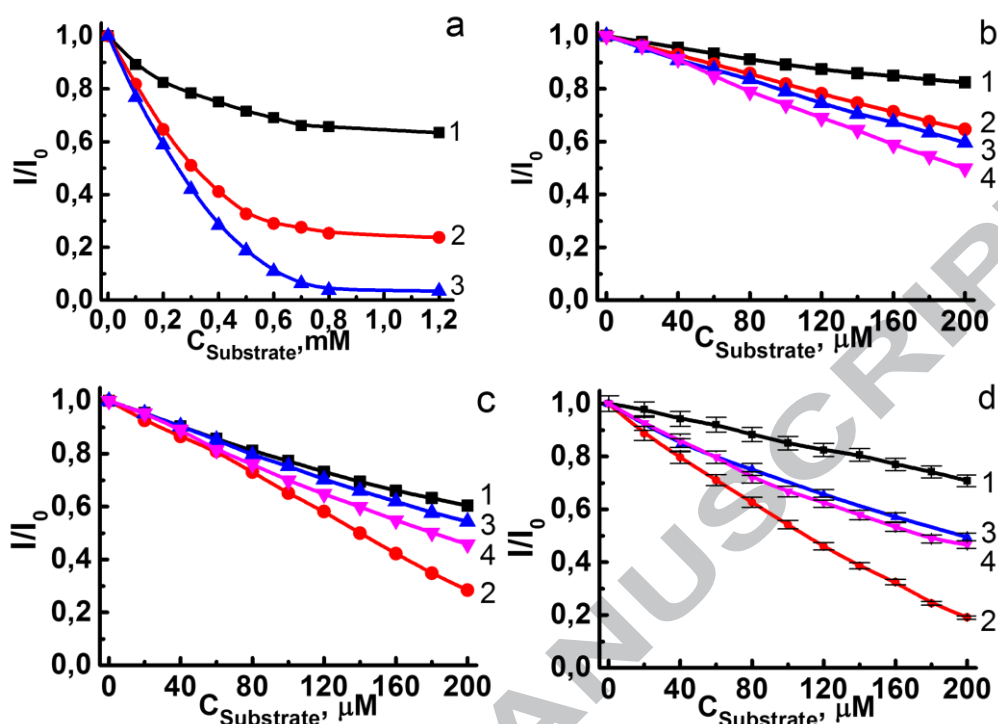


**Fig. 6.**  $I/I_0$  values at 505 nm ( $\lambda_{ex}=365$  nm) of PEI-(AuCl)<sub>2</sub>L colloids (0.4 mM) versus concentration of substrates: G-SH (1); DTT (2); Cys (3); Hcy (4) where  $I_0$  and  $I$  refers to intensity of the colloids before and after the substrate addition correspondingly. The data in wide concentration range without adjusting pH value (a); the same data in the narrow concentration range (b); the data, when pH was adjusted by MES to 5.6 (c) and 6.8 (d), where standard deviations are shown as standard bars.

The discussion of thiol-mediated luminescence response of PEI-(AuCl)<sub>2</sub>L colloids should be preceded by the data revealing another factors, such as pH, buffer or some well-known chelating anions influencing the luminescence of the colloids. The obtained results indicate that the luminescence of PEI-(AuCl)<sub>2</sub>L remains unchanged within pH 5.0-7.5 (Fig.S3, Suppl. Mat.) and in wide concentration range of Na<sub>2</sub>EDTA (Fig.S4, Suppl. Mat.). These data indicate the lack of the stripping effect of ethylenediaminetetraacetate anions. Moreover, the presence of ascorbate anions which are well-known reducing agents in synthesis of gold nanoparticles results in rather small quenching effect on the emission of PEI-(AuCl)<sub>2</sub>L instead of their whole degradation (Fig.S4, Suppl. Mat.).

Stability of the luminescence of PEI-(AuCl)<sub>2</sub>L colloids in blood serum is important prerequisite for their bioanalytical application. Buffer (DPBS) solutions

of bovine serum albumin (BSA) are commonly applied as a simplest model of blood plasma. It is worth noting that the luminescence of PEI-(AuCl)<sub>2</sub>L remains unchanged in DPBS-based solution of BSA (Fig.S5, Suppl. Mat.). Cysteine residues are worth noting as common component of the proteins, although they are regarded as the least exposed residue in proteins due to great extent of burial and clustering of the cysteine residues within proteins [32]. The lack of the luminescent response on BSA is in good agreement with the structure of BSA. Moreover, this result argues for the applicability of PEI-(AuCl)<sub>2</sub>L in bioanalysis.

Both reducing and complexing ability of thiols should induce a stripping of Au(I) ions from PEI-(AuCl)<sub>2</sub>L nanoparticles. Indeed, the increase in the concentration of thiols exemplified by cysteine (Cys), homocysteine (Hcy), glutathione (G-SH) and dithiothreitol (DTT) result in the concentration-dependent quenching of the luminescence in PEI-(AuCl)<sub>2</sub>L colloids (Fig. 6 a,b). The plotting of the quenching data as relative intensity ( $I/I_0$ , where  $I_0$  and  $I$  are the colloids luminescence intensity before and after addition of thiols) versus thiol concentration (Fig.6a) indicates that the quenching extent dramatically depends on the structure of thiol. In particular, the thiol-induced quenching of PEI-(AuCl)<sub>2</sub>L luminescence tends to increase in the following sequence  $G-SH < DTT < Cys$  (Fig.6a). The measurements represented in Figs. 6 a,b were done in nonbuffered conditions in order to reveal the acidification of the solution resulted from the thiol-induced quenching. Indeed, pH is about 5.6 in the initial colloid solution, while tends to continuously decrease to 3.6-4.0 at 200  $\mu$ M of the thiols (for more details see Table S1, Suppl. Mat.). Thus, the quenching derives from the process, which can be schematically represented by equilibrium (2), followed by further transformation of AuSR due to high redox activity of Au<sup>+</sup> and RS<sup>-</sup>. The equilibrium (3) producing Au<sup>0</sup> and the disulfide can be assumed as the result of the transformation.



The appearance of emission at  $\sim$ 420 nm as the additional shoulder at the wide emission band of (AuCl)<sub>2</sub>L in PEI-(AuCl)<sub>2</sub>L colloids after the addition of the thiols (Fig. S6, Suppl. Mat.) can be explained by surface plasmon resonance

emission band arisen from the formation of  $\text{Au}^0$  nanoparticles in the thiol-containing solutions. The solution acidification confirms the protons deliverance due to equilibrium (2) and shifts the equilibrium (2) to the left. Thus, pH of the solutions of PEI-(AuCl)<sub>2</sub>L was adjusted to various levels in order to affect the quenching effect of the thiols, since the pH is the reason for shifting of the equilibrium (2). The shifting, in turn, is the reason for influence on the luminescent response to the biothiols.

Indeed, the quenching effect of the thiols increased when the measurements were performed in the buffer solutions at pH 5.6 and 6.8 (Figs. 6 c,d). pH 6.8 provides optimal conditions for the greatest deviation between concentration dependencies of  $I/I_0$  for G-SH, Cys and DTT, while the quenching effects induced by Cys and Hcy are very similar. The greatest quenching effect of DTT (Fig.6 d) is in good agreement with its enhanced complexing ability versus Cys and G-SH due to the presence of two SH groups [33-36]. The insignificant effect of methionine possessing C-S-CH<sub>3</sub> moiety instead of SH group on the colloids emission (Fig.S4, Suppl. Mat.) points to the impact of the latter on the quenching effect of the thiols. This result along with the small quenching effect of ascorbate anions (Fig. S4 in Suppl. Mat.) confirms that the complex formation of the thiols with  $\text{Au}^+$  ions due to equilibrium (2) is the reason for their stripping from the colloids. It is also worth noting that Cys and Hcy mediate more enhanced quenching than G-SH.

The core-shell nano-architecture of PEI-(AuCl)<sub>2</sub>L, in particular the PEI-based exterior layer, is worth noting as the factor affecting the fluorescence response of (AuCl)<sub>2</sub>L on the tiols. It is in particular well-known that a charge of exterior layer commonly plays a crucial role in a luminescent response of core-shell colloids [27-29]. Thus, PEI-based adlayer of PEI-(AuCl)<sub>2</sub>L is worth noting as a factor favoring the luminescence response on anions versus cations, although the heterogeneous nature of the colloids can be a reason for a time-dependent luminescent response. The luminescence response of PEI-(AuCl)<sub>2</sub>L colloids was measured at different time duration after the sample preparation. The obtained data (Fig.S7a,b in Suppl. Mat.) indicate that the quenching effect of Cys and G-SH tend to increase within ten minutes. Nevertheless, the immediate (within one minute) measurements provide better linearity of  $I/I_0$  versus concentration of Cys, Hcy and G-SH at pH 6.8 (Fig.6d) than the similar dependence on the basis of the

measurements performed within ten minutes after the sample preparation (Fig.6, Fig.S7c in Suppl. Mat.).

The represented data are enough to reveal the origin and regularities of the thiol-mediated luminescence response of PEI-(AuCl)<sub>2</sub>L, while the detection conditions should be optimized for the lower detection level of the thiols.

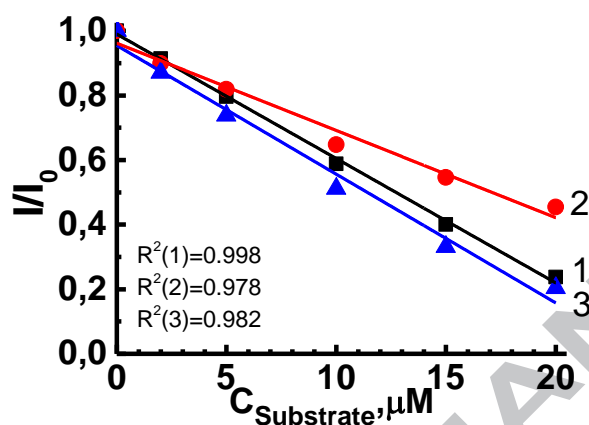


**Fig. 7.** Linear relationships between  $I/I_0$  at 505 nm ( $\lambda_{\text{ex}}=365$  nm) of PEI-(AuCl)<sub>2</sub>L colloids (0.04 mM) and thiols concentration: Cys (1); G-SH (2); Hcy (3). Coefficient of determination ( $R^2$ ) is presented in the plot, slope (b) and intercept (a) values are presented in Table S2 in Suppl. Mat.

Figure 7 represents the luminescence response of PEI-(AuCl)<sub>2</sub>L on Cys, Hcy and G-SH in the narrow concentration range 0-20  $\mu\text{M}$  of the thiols. The results (Fig.7) indicate no significant difference in the quenching effect of Cys, Hcy and G-SH within 0-5  $\mu\text{M}$  of the thiols. Deviation between the  $I/I_0$  values plotted versus Cys and G-SH concentration tends to increase within 5-20  $\mu\text{M}$ , which results in better linearity of the plot for Cys versus G-SH (Fig.7, Table 1). Taking into account that relative standard deviation of  $I/I_0$  values lies within 1-1.5 % the lower detection limit of Cys, Hcy and G-SH is about 1  $\mu\text{M}$  (Table 1). Table 1 represents the lower detection (LD) and linear range (LR) values both estimated in the present work and taken from the literature data. The obtained results (Table 1) highlight PEI-(AuCl)<sub>2</sub>L colloids as good (not the best) sensors on the biothiols without significant discrimination between them within the 0-5  $\mu\text{M}$  concentration range.

It is also worth noting that high affinity of G-SH to PEI-(AuCl)<sub>2</sub>L makes the latter very promising basis for affecting the so-called ROS level in living cells due to the well-known impact of G-SH on the maintaining optimal ROS level [37]. This task lies out of the present work scope but will be studied in a nearest future and represented elsewhere.

**Table 1.** Comparison of various sensors for biothiols detection using fluorescence technique: LD and LR values calculated from data obtained in the present work and taken from literature data.

Materials used	Thiols	LR	LD	Ref.
Fe quantum clusters incorporated into Hb/Zn(II) complex	Cys	1-20 $\mu$ M	0.25 $\mu$ M	[38]
Triethylenetetramine modified CDs/Cu(II) complex	G-SH	0.2-175 $\mu$ M	0.11 $\mu$ M	[39]
N,S- doped CDs loaded with Cu(II)	Cys	0-11 $\mu$ M	86nM	[40]
	Hcy		86nM	
	G-SH		86nM	
N-doped CDs	G-SH	0.2-1000 $\mu$ M	30nM	[41]
Single-stranded DNA stabilized Ag NCs/Hg <sup>2+</sup> system	Cys	0.1-0.6 $\mu$ M	1.59nM	[42]
	G-SH	0.1-0.5 $\mu$ M	2.88nM	
HSA-stabilized Au/Ag core/shell NCs	Cys and Hcy (total)	0.1-5 $\mu$ M	15nM	[43]
Graphene QDs coupled to Au NPs	Cys	1-4 $\mu$ M	0.32nM	[44]
Au@Ag nanoclusters	Cys	0.02-80 $\mu$ M	5.87nM	[16]
	G-SH	2-70 $\mu$ M	1.01 $\mu$ M	
Au NPs decorated reduced graphene oxide nanohybrid	Cys	0-3nM	0.51nM	[45]
GSH-Au NCs/ Ag <sup>+</sup> system	Cys	0-2.71 $\mu$ M	16.54nM	[46]
N,S- doped CDs/AuNPs	G-SH	0.01-5 $\mu$ M	3.6nM	[47]
PEI-[(AuCl) <sub>2</sub> L] colloids	Cys	0-20 $\mu$ M	1 $\mu$ M	This work
	Hcy	0-20 $\mu$ M	1 $\mu$ M	
	G-SH	0-20 $\mu$ M	1 $\mu$ M	

## Conclusions

The present work for the first time highlights facile synthetic approach for conversion of luminescent Au(I) complex (AuCl)<sub>2</sub>L with poor stability in solutions into stable in time hydrophilic colloids as the nanosensors for biothiols.

Dissociation of  $(\text{AuCl})_2\text{L}$  is one of the reasons for its instability in solutions. Both deposition of PEI on  $(\text{AuCl})_2\text{L}$ -based nanoparticles and the presence of NaCl as an ionic background are the factors restricting the dissociation of  $(\text{AuCl})_2\text{L}$ . This is the reason for significant stability of  $(\text{AuCl})_2\text{L}$  in the synthesized core-shell colloids. In particular, the luminescence of the colloids arisen from the emission of  $(\text{AuCl})_2\text{L}$  remains unchanged within one week at least. No changes in the luminescence is observed in the solutions of ethylenediaminetetraacetate and ascorbate anions, as well as in saline buffer solutions of bovine serum albumin. The concentration- and pH-dependent quenching of PEI- $(\text{AuCl})_2\text{L}$  emission is revealed in the solutions of thiols and biothiols. The stripping effect of SH groups plays a key role in the luminescence response of PEI- $(\text{AuCl})_2\text{L}$ . The present work introduces the recognition of cysteine, homocysteine and glutathione versus methionine by luminescent response of PEI- $(\text{AuCl})_2\text{L}$  which highlights the synthesized colloids as promising for bioanalytical and biomedical purposes.

#### Compliance with ethical standards

The author(s) declare that they have no competing interests.

#### References

- [1] X. He, V. W.-W. Yan, Luminescent gold(I) complexes for chemosensing, *Coord. Chem. Rev.* 255 (2011) 2111–2123.
- [2] J. Lima, L. Rodriguez, Applications of gold(I) alkynyl systems: a growing field to explore, *Chem. Soc. Rev.* 40 (2011) 5442–5456.
- [3] Q. Zhao, C. Huanga, F. Li, Phosphorescent heavy-metal complexes for bioimaging, *Chem. Soc. Rev.* 40 (2011) 2508–2524.
- [4] P.K. Upadhyay, S.B. Marpu, E.N. Benton, C.L. Williams, A. Telang, M.A. Omary, A Phosphorescent Trinuclear Gold(I) Pyrazolate Chemosensor for Silver Ion Detection and Remediation in Aqueous Media, *Anal. Chem.* 90 (2018) 4999-5006.
- [5] J. Liang, Z. Chen, L. Xu, J. Wang, J. Yin, G.-A. Yu, Z.-N. Chen, Z. H. Liu, Aggregation-induced emission-active gold(I) complexes with multi-stimuli luminescence switching, *J. Mater. Chem. C* 2 (2014) 2243–2250.

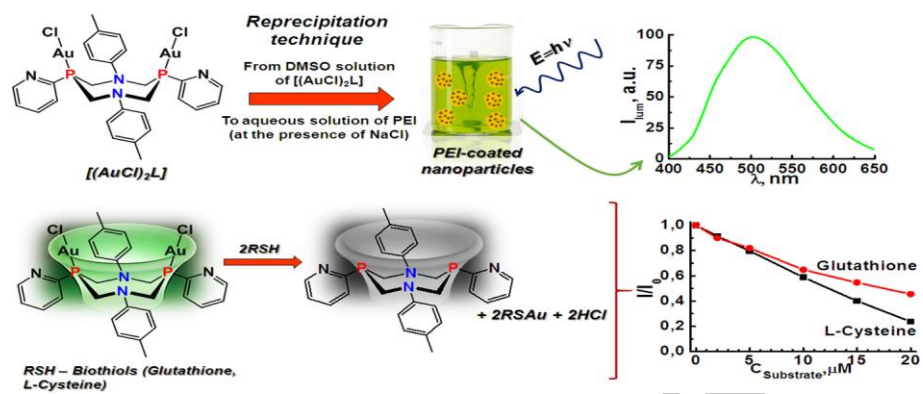
- [6] Y. Yu, J. Yang, X. Xu, Y. Jiang, B. Wang, A novel fluorescent probe for highly sensitive and selective detection of cysteine and its application in cell imaging, *Sens. Actuators B* 251 (2017) 902–908.
- [7] Y. Wang, M. Zhu, E. Jiang, R. Hua, R. Na, Q. X. Li, A Simple and Rapid Turn On ESIPT Fluorescent Probe for Colorimetric and Ratiometric Detection of Biothiols in Living Cells, *Sci. Rep.* 7 (2017) 4377.
- [8] Y. Shen, X. Zhang, Y. Zhang, Ch. Zhang, J. Jin, H. Li, A new simple phthalimide-based fluorescent probe for highly selective cysteine and bioimaging for living cells, *Spectrochim. Acta A* 185 (2017) 371–375.
- [9] Y. Yang, H. Wang, Y-L. Wei, J. Zhou, J-F. Zhang, Y. Zhou, A selective coumarin-based “turn-on” fluorescent sensor for the detection of cysteine and its applications for bioimaging, *Chin. Chem. Lett.* 28 (2017) 2023–2026.
- [10] C. Yin, W. Zhang, T. Liu, J. Chao, F. Huo, A near-infrared turn on fluorescent probe for biothiols detection and its application in living cells, *Sens. Actuators B* 246 (2017) 988–993.
- [11] Z. Xue, X. Fu, H. Rao, M. H. Ibrahim, L. Xiong, X. Liu, X. Lu, A colorimetric indicator-displacement assay for cysteine sensing based on a molecule-exchange mechanism, *Talanta* 174 (2017) 667–672.
- [12] Z. A. Tehrani, Z. Jamshidi, M. J. Javan, A. Fattahi, Interactions of Glutathione Tripeptide with Gold Cluster: In fluence of Intramolecular Hydrogen Bond on Complexation Behavior, *J. Phys. Chem. A* 116 (2012) 4338–4347.
- [13] F. X. Zhang, L. Han, L. B. Israel, J. G. Daras, M. M. Maye, N. K. Ly, Ch-J. Zhong, Colorimetric detection of thiol-containing amino acids using gold nanoparticles, *Analyst* 127 (2002) 462–465.
- [14] L. Hu, S. Hu, L. Guo, T. Tang, M. Yang, Optical and electrochemical detection of biothiols based on aggregation of silver nanoparticles, *Anal. Methods* 8 (2016) 4903–4907.
- [15] X. Su, H. Jiang, X. Wang, Thiols-Induced Rapid Photoluminescent Enhancement of Glutathione-Capped Gold Nanoparticles for Intracellular Thiols Imaging Applications, *Anal. Chem.* 87 (2015) 10230–10236.

- [16] Z.-X. Wang, S.-N. Ding, E. Y. J. Narjh, Determination of Thiols by Fluorescence using Au@Ag Nanoclusters as Probes, *Anal. Lett.* 48 (2015) 647–658.
- [17] F. Ghasemi, M. R. Hormozi-Nezhad, M. Mahmoudi, A colorimetric sensor array for detection and discrimination of biothiols based on aggregation of gold nanoparticles, *Anal. Chim. Acta* 882 (2015) 58–67.
- [18] J.-F. Li, P.-Ch. Huang, F.-Y. Wu, Highly selective and sensitive detection of glutathione based on anti-aggregation of gold nanoparticles via pH regulation, *Sens. Actuators B* 240 (2017) 553–559.
- [19] Z.-J. Li, X.-J. Zheng, L. Zhang, R.-P. Liang, Z.-M. Li, J.-D. Qiu, Label-free colorimetric detection of biothiols utilizing SAM and unmodified Au nanoparticles, *Biosens. Bioelectron.* 68 (2015) 668–674.
- [20] L. Ji, J. Wang, L. Zhu, Y. Zu, J. Kong, Z. Chen, Differentiation of biothiols from other sulfur-containing biomolecules using iodide-capped gold nanoparticles, *RSC Adv.* 6 (2016) 25101–25109.
- [21] M. Shahrajabian, R. Hormozi-Nezhad, Design a New Strategy Based on Nanoparticle-Enhanced Chemiluminescence Sensor Array for Biothiols Discrimination, *Sci. Rep.* 6 (2016) 32160.
- [22] I. Strel'nik, V. Gurzhiy, V. Sizov, E. Musina, A. Karasik, S. Tunik, E. Grachova, A stimuli-responsive Au(I) complex based on an aminomethylphosphine template: synthesis, crystalline phases and luminescence properties, *CrystEngComm* 18 (2016) 7629–7635.
- [23] N. Shamsutdinova, I. Strel'nik, E. Musina, T. Gerasimova, S. Katsyuba, V. Babaev, D. Krivolapov, I. Litvinov, A. Mustafina, A. Karasik, O. Sinyashin, “Host–guest” binding of a luminescent dinuclear Au(I) complex based on cyclic diphosphine with organic substrates as a reason for luminescence tuneability, *New J. Chem.* 40 (2016) 9853–9861.
- [24] A.V. Delgado, F. Gonzalez-Caballero, R.J. Hunter, L.K. Koopal, J. Lyklema, Measurement and interpretation of electrokinetic phenomena, *J. Colloid Int. Sci.* 309 (2007) 194–224.
- [25] DIFFRAC Plus Evaluation package EVA, Version 11, User's Manual, Bruker AXS, Karlsruhe, Germany, **2005**, 258 p.

- [26] TOPAS V3: General profile and structure analysis software for powder diffraction data. **2005**, Technical Reference. Bruker AXS. Karlsruhe. Germany.- 117 p.
- [27] N. Davydov, R. Zairov, A. Mustafina, V. Syakayev, A. Konovalov, M. Mustafin, Determination of fluoroquinolone antibiotics through the fluorescent response of Eu (III) based nanoparticles fabricated by layer-by-layer technique, *Anal. Chim. Acta* 784 (2013) 65–71.
- [28] N. Shamsutdinova, R. Zairov, A. Mustafina, S. Podyachev, Physicochemical and Engineering Aspects Interfacial interactions of hard polyelectrolyte-stabilized luminescent colloids with substrates, *Colloids Surf. A* 482 (2015) 231–240.
- [29] N. Shamsutdinova, R. Zairov, I. Nizameev, A. Gubaidullin, A. Mukhametshina, S. Podyachev, I. Ismayev, M. Kadirov, A. Voloshina, T. Mukhametzhanov, A. Mustafina, Tuning magnetic relaxation properties of “hard cores” in core-shell colloids by modification of “soft shell”, *Colloids Surf. B* 162 (2018) 52–59.
- [30] R. Zairov, A. Mustafina, N. Shamsutdinova, I. Nizameev, B. Moreira, S. Sudakova, S. Podyachev, A. Fattakhova, G. Safina, I. Lundstrom, A. Gubaidullin, A. Vomiero, High performance magneto-fluorescent nanoparticles assembled from terbium and gadolinium 1,3-diketones, *Sci. Rep.* 7 (2017) 40486.
- [31] V. Izumrudov, E. Kharlampieva, S. A. Sukhishvili, Salt-induced multilayer growth: correlation with phase separation in solution, *Macromolecules* 37 (2004) 8400–8406.
- [32] L.B. Poole, The Basics of Thiols and Cysteines in Redox Biology and Chemistry, *Free Radic. Biol. Med.* 80 (2015) 148–157.
- [33] W. Cleland, Dithiothreitol, a new protective reagent for SH groups, *Biochemistry* 3 (1964) 480–482.
- [34] M.J. O'Neil, *An encyclopedia of chemicals, drugs, & biological*, United States, 2001.
- [35] A. Rigo, A. Corazza, M. L. di Paolo, M. Rossetto, R. Ugolini, M. Scarpa, Interaction of copper with cysteine: stability of cuprous complexes and catalytic role of cupric ions in anaerobic thiol oxidation, *J. Inorg. Biochem.* 98 (2004) 1495–1501.

- [36] D. Du, J. Ding, Y. Tao, X. Chen, Application of chemisorption/desorption process of thiocholine for pesticide detection based on acetylcholinesterase biosensor, *Sens. Actuators B* 134 (2008) 908–912.
- [37] M.H. Raza, S. Siraj, A. Arshad, U. Waheed, F. Aldakheel, S. Alduraywish, M. Arshad, ROS-modulated therapeutic approaches in cancer treatment, *J. Cancer Res. Clin. Oncol.* 143 (2017) 1789–1809.
- [38] N. Hashemi, Z. Vaezi, M. Sedghi, H. Naderi-Manesh, Hemoglobin-incorporated iron quantum clusters as a novel fluorometric and colorimetric probe for sensing and cellular imaging of Zn(II) and cysteine, *Microchim. Acta* 185 (2018) 60.
- [39] R. Yang, X. Guo, L. Jia, Y. Zhang, A fluorescent “on-off-on” assay for selective recognition of Cu(II) and glutathione based on modified carbon nanodots, and its application to cellular imaging, *Microchim. Acta* 184 (2017) 1143–1150.
- [40] Y. Guo, L. Yang, W. Li, X. Wang, Y. Shang, B. Li, Carbon dots doped with nitrogen and sulfur and loaded with copper(II) as a “turn-on” fluorescent probe for cystein, glutathione and homocysteine, *Microchim. Acta* 183 (2016) 1409–1416.
- [41] D. Wu, G. Li, X. Chen, N. Qiu, X. Shi, G. Chen, Z. Sun, J. You, Y. Wu, Fluorometric determination and imaging of glutathione based on a thiol-triggered inner filter effect on the fluorescence of carbon dots, *Microchim. Acta* 184 (2017) 1923–1931.
- [42] Z.Y. Yan, C. Tian, X. Sun, Y. Wu, D. Li, B. Ye, Ratiometric detection of biothiols by using the DNA-templated silver nanoclusters–Hg<sup>2+</sup> system, *Anal. Methods* 10 (2018) 706–712.
- [43] R. Gui, Y. Wang, J. Sun, Protein-stabilized fluorescent nanocrystals consisting of a gold core and a silver shell for detecting the total amount of cysteine and homocysteine, *Microchim. Acta* 181 (2014) 1231–1238.
- [44] S. Huang, L. Wang, C. Huang, B. Hu, W. Su, Q. Xiao, Graphene quantum dot coupled with gold nanoparticle based “off-on” fluorescent probe for sensitive and selective detection of L-cysteine, *Microchim. Acta* 183 (2016) 1855–1864.

- [45] B. Thirumalraj, N. Dhenadhayalan, S.-M. Chen, Y.-J. Liu, T.-W. Chen, P.-H. Liang, K.-C. Lin, Highly sensitive fluorogenic sensing of L-Cysteine in live cells using gelatin-stabilized gold nanoparticles decorated graphene nanosheets, *Sens. Actuators B* 259 (2018) 339–346.
- [46] Y. Li, Y. Deng, X. Zhou, J. Hu, A label-free turn-on-off fluorescent sensor for the sensitive detection of cysteine via blocking the Ag<sup>+</sup> - enhancing glutathione-capped gold nanoclusters, *Talanta* 179 (2018) 742–752.
- [47] J. Li, X. Rao, F. Xiang, J. Wei, M. Yuan, Z. Liu, A photoluminescence “switch-on” nanosensor composed of nitrogen and sulphur co-doped carbon dots and gold nanoparticles for discriminative detection of glutathione, *Analyst* 143 (2018) 2083–2089.



[48]

ACCEPTED MANUSCRIPT

Synthesis of aqueous core-shell luminescent colloids for sensing of thiols  
Au(I) complex as basis for hard cores coated by soft polyelectrolyte shell  
Specific interactions at core/shell interface provide stability of colloids  
pH-dependent quenching effects of thiols on colloids luminescence  
Thiol-induced stripping of Au<sup>+</sup> ions from colloids is a reason for the quenching

[49]

ACCEPTED MANUSCRIPT